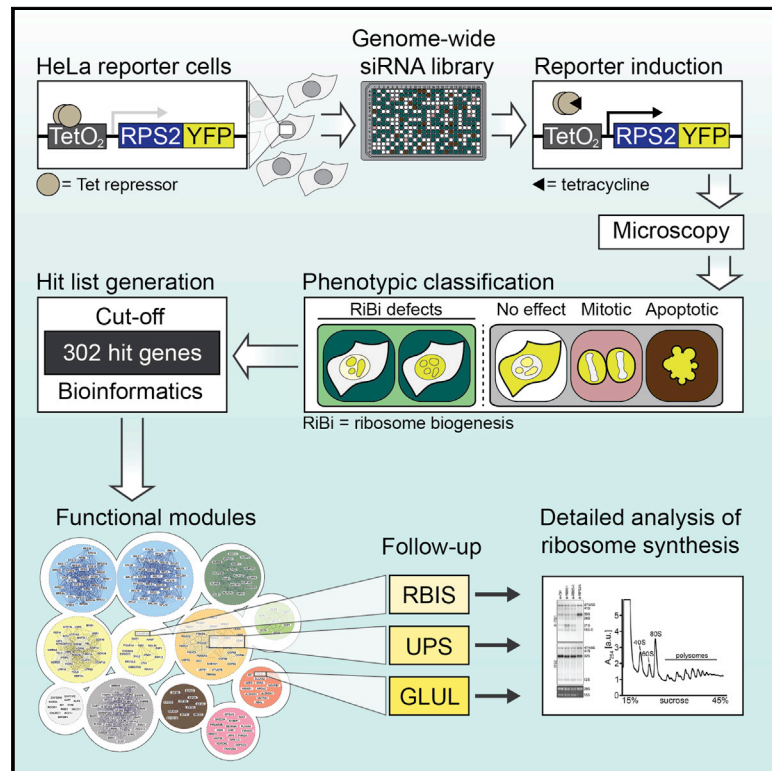# Genome-wide RNAi Screening Identifies Protein Modules Required for 40S Subunit Synthesis in Human Cells

Graphical Abstract

Authors

Lukas Badertscher, Thomas Wild, Christian Montellese, ..., Ivo Zemp, Peter Horvath, Ulrike Kutay

Correspondence

ulrike.kutay@bc.biol.ethz.ch

In Brief

Badertscher et al. perform an image-based, genome-wide RNAi screen on 40S ribosomal subunit biogenesis and identify ~300 factors that support this process in human cells. Among these are many factors belonging to essential protein modules, including the ubiquitin-proteasome system, vertebrate-specific ribosome synthesis factors such as RBIS, and the glutamine synthetase GLUL.

Highlights

- Genome-wide RNAi screening identifies ~300 factors required for 40S subunit production

- The E3 ubiquitin ligase CRL4 is required for nucleolar steps of ribosome maturation

- Intracellular Gln synthesis supports efficient nuclear maturation of 40S subunits

CrossMark

CellPress

Genome-wide RNAi Screening Identifies Protein Modules Required for 40S Subunit Synthesis in Human Cells

Lukas Badertscher,[1,5] Thomas Wild,[1,6] Christian Montellese,[1,5] Leila T. Alexander,[2] Lukas Bammert,[1,5] Marie Sarazova,[1,5] Michael Stebler,[3] Gabor Csucs,[3] Thomas U. Mayer,[4] Nicola Zamboni,[2] Ivo Zemp,[1] Peter Horvath,[1,3,7] and Ulrike Kutay[1,*]
[1]Institute of Biochemistry, ETH Zurich, 8093 Zurich, Switzerland
[2]Institute of Molecular Systems Biology, ETH Zurich, 8093 Zurich, Switzerland
[3]RNAi Screening Center, ScopeM, ETH Zurich, 8093 Zurich, Switzerland
[4]Department of Biology, University of Konstanz, 78457 Konstanz, Germany
[5]Molecular Life Sciences Ph.D. Program, 8057 Zurich, Switzerland
[6]Present address: The Novo Nordisk Foundation Center for Protein Research, University of Copenhagen, 2200 Copenhagen, Denmark
[7]Present address: Synthetic and Systems Biology Unit, Biological Research Center, 6726 Szeged, Hungary
*Correspondence: ulrike.kutay@bc.biol.ethz.ch
http://dx.doi.org/10.1016/j.celrep.2015.11.061

SUMMARY

Ribosome biogenesis is a highly complex process requiring many assisting factors. Studies in yeast have yielded comprehensive knowledge of the cellular machinery involved in this process. However, many aspects of ribosome synthesis are different in higher eukaryotes, and the global set of mammalian ribosome biogenesis factors remains unexplored. We used an imaging-based, genome-wide RNAi screen to find human proteins involved in 40S ribosomal subunit biogenesis. Our analysis identified ~300 factors, many part of essential protein modules such as the small subunit (SSU) processome, the eIF3 and chaperonin complexes, and the ubiquitin-proteasome system. We demonstrate a role for the vertebrate-specific factor RBIS in ribosome synthesis, uncover a requirement for the CRL4 E3 ubiquitin ligase in nucleolar ribosome biogenesis, and reveal that intracellular glutamine synthesis supports 40S subunit production.

INTRODUCTION

Ribosomes are conserved molecular machines dedicated to protein synthesis in all kingdoms of life. They are built from a small and a large subunit, both of which are sophisticated ribonucleoprotein particles composed of rRNA and ribosomal proteins (RPs). Although the ribosome structure and mode of operation follow the same principles in all species, ribosome synthesis has become more complex during evolution. The reasons for this greater complexity include increases in ribosome size, the establishment of nucleo-cytoplasmic compartmentalization, and the evolution of elaborate signaling networks that control ribosome synthesis and function, especially

in higher eukaryotes. Importantly, deregulated ribosome production is associated with various ribosomopathies and cancer (Bywater et al., 2013; Hannan et al., 2013; Stumpf and Ruggero, 2011; Teng et al., 2013).

In vertebrates, the small 40S ribosomal subunit contains one rRNA (18S) and 33 ribosomal proteins (RPSs), whereas the large 60S subunit is built of three rRNAs (28S, 5.8S, and 5S) and 47 ribosomal proteins (RPLs). Ribosomal subunit biogenesis begins in specialized nuclear regions, called nucleoli, that are organized around repeats of rRNA genes. RNA polymerase I (Pol I) transcribes these genes as long precursor rRNAs (pre-rRNAs). Each pre-rRNA contains rRNA segments (18S, 5.8S, and 28S) that are surrounded by RNA regions that are removed in a number of temporally and spatially controlled rRNA processing reactions. Concomitant with rRNA transcription and processing, the pre-rRNA is modified by pseudouridylation and methylation, mostly catalyzed by a large number of small nucleolar ribonucleoprotein (snoRNP) particles. The process of rRNA maturation is tightly coupled to the ordered deposition of ribosomal proteins onto the pre-rRNA. An endonucleolytic cleavage step splits the nascent pre-ribosome into the precursors of 40S and 60S subunits in the nucleolus, which, thereafter, follow separate biogenesis pathways. Pre-60S maturation also includes the incorporation of 5S rRNA, which is synthesized independently by RNA Pol III. Following further nuclear biogenesis steps and nuclear export, pre-40S and pre-60S particles are finally matured in the cytoplasm, where both subunits join to form the translationally competent 80S ribosome. In yeast, the whole process of ribosome production is assisted by >200 non-ribosomal proteins known as *trans*-acting factors (Henras et al., 2008; Thomson et al., 2013; Tschochner and Hurt, 2003; Turowski and Tollervey, 2015; Woolford and Baserga, 2013).

Ribosome synthesis is an energy-demanding process that is tightly regulated and occupies a central position in growth control (Drygin et al., 2010; Warner, 1999). To adapt ribosome production to cellular needs, vertebrate cells integrate a large variety of upstream cues, including nutrient availability. Defects in

ribosome synthesis, in turn, are relayed into elaborate stress response pathways, such as p53 activation, that ensure cellular and organismal homeostasis (Deisenroth and Zhang, 2010).

Although ribosome biogenesis in yeast has been studied intensively, little is known about this process in vertebrate cells in comparison. Recently, we and others took the first systematic approaches to identify factors involved in ribosome biogenesis in human cells by performing candidate RNAi screens on human homologs of yeast ribosome synthesis factors and a subset of nucleolar proteins, respectively (Tafforeau et al., 2013; Wild et al., 2010). These screens revealed that basic aspects of the process are conserved between yeast and mammals. However, important dissimilarities in ribosome synthesis exist between fungi and humans, caused by differences in the genomic organization of rDNA, rRNA maturation, subunit size, and regulation.

To shed light on the cellular machinery required for 40S synthesis in human cells, we performed a genome-wide, image-based siRNA screen yielding a high confidence group of proteins required for small subunit biogenesis. Many of the identified genes have been linked to disease, emphasizing the importance of balanced ribosome synthesis for organismal homeostasis. To demonstrate the utility of this dataset, we focused our follow-up analyses on three factors without a characterized role in ribosome production: ribosome biogenesis factor identified in screen (RBIS), a vertebrate-specific ribosome biogenesis factor; a protein module belonging to the ubiquitin-proteasome system, revealing a link between the cullin 4 E3 ubiquitin ligase and human ribosome synthesis; and GLUL, an enzyme that converts glutamate into glutamine. Collectively, our dataset not only provides a collection of references for research on human ribosome biogenesis but also a rich source for deciphering connections between diverse cellular pathways and ribosome synthesis—an anabolic pillar that is central to life.

RESULTS AND DISCUSSION

siRNA Screening Identifies 302 Factors Required for 40S Subunit Synthesis

To identify factors involved in the synthesis of human 40S ribosomal subunits by imaging-based RNAi screening, we used a previously established HeLa cell line expressing a tetracycline-inducible RPS2-yellow fluorescent protein (YFP) reporter (Wild et al., 2010; Zemp et al., 2009). After induction, newly synthesized RPS2-YFP is imported into the nucleus, assembled into pre-ribosomes in the nucleolus, and exported along with freshly made subunits back into the cytoplasm. In our assay, reporter cells were first treated with siRNAs for 58 hr before the expression of RPS2-YFP was induced for 14 hr, allowing us to monitor the effect of protein depletion on the biogenesis of newly synthesized 40S subunits (Figure 1A).

In control cells, RPS2-YFP localized to the cytoplasm, mostly as part of mature 40S subunits (Zemp et al., 2009), and was also found in nucleoli, where it joins nascent subunits (Figure 1B). Loss of cytoplasmic localization accompanied by nuclear accumulation of the reporter was exploited for quantification of siRNA-induced defects in 40S biogenesis. Based on distinct patterns of nuclear localization of the RPS2-YFP reporter, we could distinguish two different phenotypes: nucleolar accumulation of

RPS2-YFP caused by early ribosome maturation defects (e.g., upon depletion of fibrillarin [si-FBL], a box C/D snoRNP-associated methyltransferase) and nucleoplasmic accumulation of RPS2-YFP resulting from nucleoplasmic maturation or export defects (e.g., induced by downregulation of the pre-40S exportin XPO1/CRM1 [si-XPO1]) (Figure 1B).

For automated data analysis, images were segmented based on Hoechst staining of cell nuclei, and diverse features were extracted, including nuclear and cytoplasmic fluorescence intensities, with a customized version of CellProfiler (Carpenter et al., 2006). Supervised machine learning was applied to assign cells into predefined phenotypic classes. These categories included cells displaying 40S biogenesis defects based on the subcellular localization of the RPS2-YFP reporter, cells without reporter expression, and mitotic or apoptotic cells. For each siRNA, a hit rate was calculated, defined as the percentage of RPS2-YFP-expressing interphase cells showing nuclear accumulation of the reporter (Wild et al., 2010).

The screening campaign was performed in two steps (Figure 1A). First, a primary screen was done on the entire genome using an siRNA library that targets ~19,600 genes with ~76,000 siRNAs (four individual siRNAs per gene). This dataset (Table S1) was used to generate a ranked list of targets based on p values determined by the redundant siRNA activity (RSA) method, a probability-based algorithm evaluating the collective activities of multiple siRNAs per gene (König et al., 2007). We provide this ranked gene list as an easy-to-read, color-coded overview of the performance of each siRNA (Table S2). Second, a validation screen was performed to confirm 1,000 selected high-ranking candidate genes (Tables S3 and S4). This screen relied on three additional individual siRNAs per target from a different vendor and was repeated independently three times. The entire dataset comprises 2,300,000 pictures containing more than 60,000,000 cells. The quality of the screening campaign was monitored based on the performance of control siRNAs (Figures S1A and S1B). Separation of negative and positive controls was excellent for both the genome-wide and the validation screens (Figures S1C and S1E), reflected by high Z' factors (Figure 1C) that serve as numeric quality measures for the screening data (Zhang et al., 1999).

To define high-confidence targets required for 40S subunit synthesis in HeLa cells, we assembled a ranked RSA hit list based on the performance of all seven siRNAs used in the genome-wide and validation screens for the 1,000 candidate genes. A cutoff was defined, taking into account the reproducibility of the three independent runs of the validation screen. Possible off-target effects were reduced by correlation of our hit list with HeLa cell proteomic datasets (Nagaraj et al., 2011; Schaab et al., 2012; Table S8). This procedure resulted in a high-confidence group of 302 final hits (pictures are available at http://www.ribosomebiogenesis.org). Ribosomal proteins of the small subunit are highly enriched in the top part of this ranked hit list (Table S5). Of the 302 hit genes from our genome-wide screen, we found ~80%, i.e., 95 of the 117 factors identified previously in our candidate screen using the RPS2-YFP readout (Figure 1D; Wild et al., 2010), supporting the quality of the genome-wide dataset. Strikingly, we could identify 207 additional factors that are important for efficient biogenesis of the
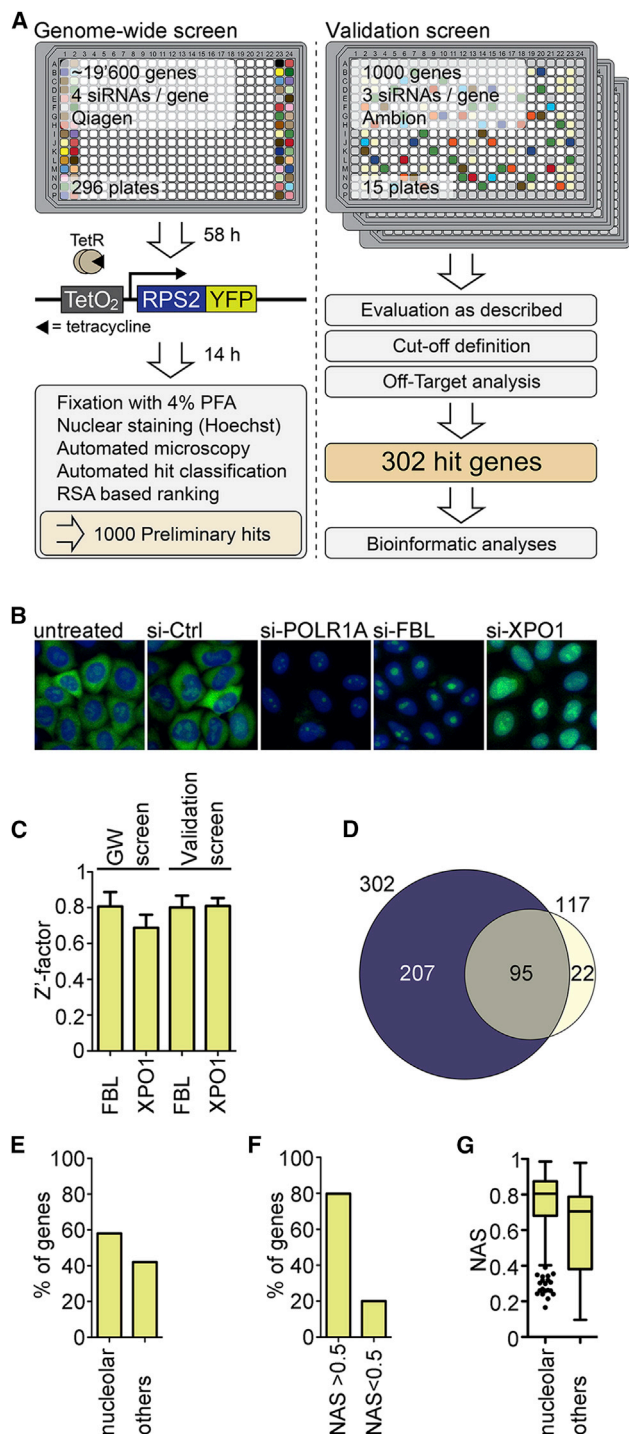
Figure 1. A Genome-wide RNAi Screen Identifies Factors Required for 40S Ribosomal Subunit Biogenesis

(A) Schematic of the screening setup. Tetracycline-inducible RPS2-YFP HeLa cells were transfected with siRNAs. 58 hr post-transfection, reporter expression was induced for 14 hr. In total, seven individual siRNAs were used per gene, four in the primary, genome-wide screen and three in each round of the validation screen, performed in triplicates.

(B) Representative screening images of different phenotypes with merged signals of RPS2-YFP (green) and Hoechst staining of nuclei (blue).

40S ribosomal subunit in the genome-wide analysis. Most of the 95 common hits between the candidate and genome-wide screen are RPs and ribosome biogenesis (RiBi) factors. Altogether, our dataset constitutes a compilation of 40S subunit biogenesis factors in humans on a genomic level.

Comparison of our hit list to the nucleolar proteome of human cells (Ahmad et al., 2009; Andersen et al., 2005; Leung et al., 2006) revealed that nucleolar proteins are highly represented in our dataset and account for about 60% of all identified factors (Figure 1E). For phenotypic classification of the hits, a nucleolar accumulation score (NAS) was calculated for each gene (Figures S1H and S1I; Table S5), defined as the ratio of cells displaying nucleolar RPS2-YFP accumulation to the total of cells with a phenotype (nucleolar and nucleoplasmic accumulation of RPS2-YFP). This phenotypic analysis demonstrated that the largest fraction of the identified factors (~80%) is involved in nucleolar steps of 40S maturation (Figures 1F and 1G). A recent screen exploring the role of 625 nucleolar proteins in pre-rRNA processing (Tafforeau et al., 2013) confirmed 55% of non-ribosomal factors derived from our previous candidate screen on 40S and 60S biogenesis and overlaps to 20% with our genome-wide analysis (Figure S1G). Although the overlap of 20% seems low at first glance, it is explained by our screen covering the entire proteome and by the differences in the focus of these screens (40S biogenesis versus rRNA processing of precursors to both subunits) in the readouts and in cutoff stringency. Furthermore, the analysis of pre-rRNA processing was population-based, whereas our screen relied on single-cell analysis accompanied by phenotypic classification of cells as the basis for hit definition.

Protein Modules Supporting 40S Subunit Biogenesis

Consistent with a function of the identified factors in ribosome biogenesis, gene ontology (GO) term enrichment analysis (Reimand et al., 2011) revealed that ribosome biogenesis, rRNA processing, and RNA binding are prominent terms in the categories of biological process and molecular function, respectively (Figure 2A), showing that the expected categories were indeed retrieved in the dataset.

To identify functional modules among the 302 hits, we used a combination of bioinformatics, exploiting GO term analysis and high-confidence protein-protein interaction networks (Franceschini et al., 2013), as well as manual literature searches. This approach created ten functional clusters (Figure 2B; Table S6). Conspicuous protein modules include RPs of both subunits and RiBi factors, reinforcing the reliability of the screening

(C) Z' factors for the positive control siRNAs directed against FBL and XPO1 as measures for the quality of the screening campaign. GW, genome-wide.

(D) Venn diagram illustrating the intersection between the 302 identified genes (purple) and 40S biogenesis factors described in a previous candidate screen (yellow; Wild et al., 2010). Both screens used the identical RPS2-YFP cell line, and 95 of the initially 117 identified factors could be validated.

(E) Fraction of identified factors previously assigned to the nucleolar proteome (Ahmad et al., 2009; Andersen et al., 2005; Leung et al., 2006).

(F) Phenotypic classification of hits based on their NAS.

(G) NAS of nucleolar proteins identified as hits shown as box plots (Tukey-style whiskers).

See also Figure S1 and Tables S1, S2, S3, S4, S5, S6, S7, and S8.
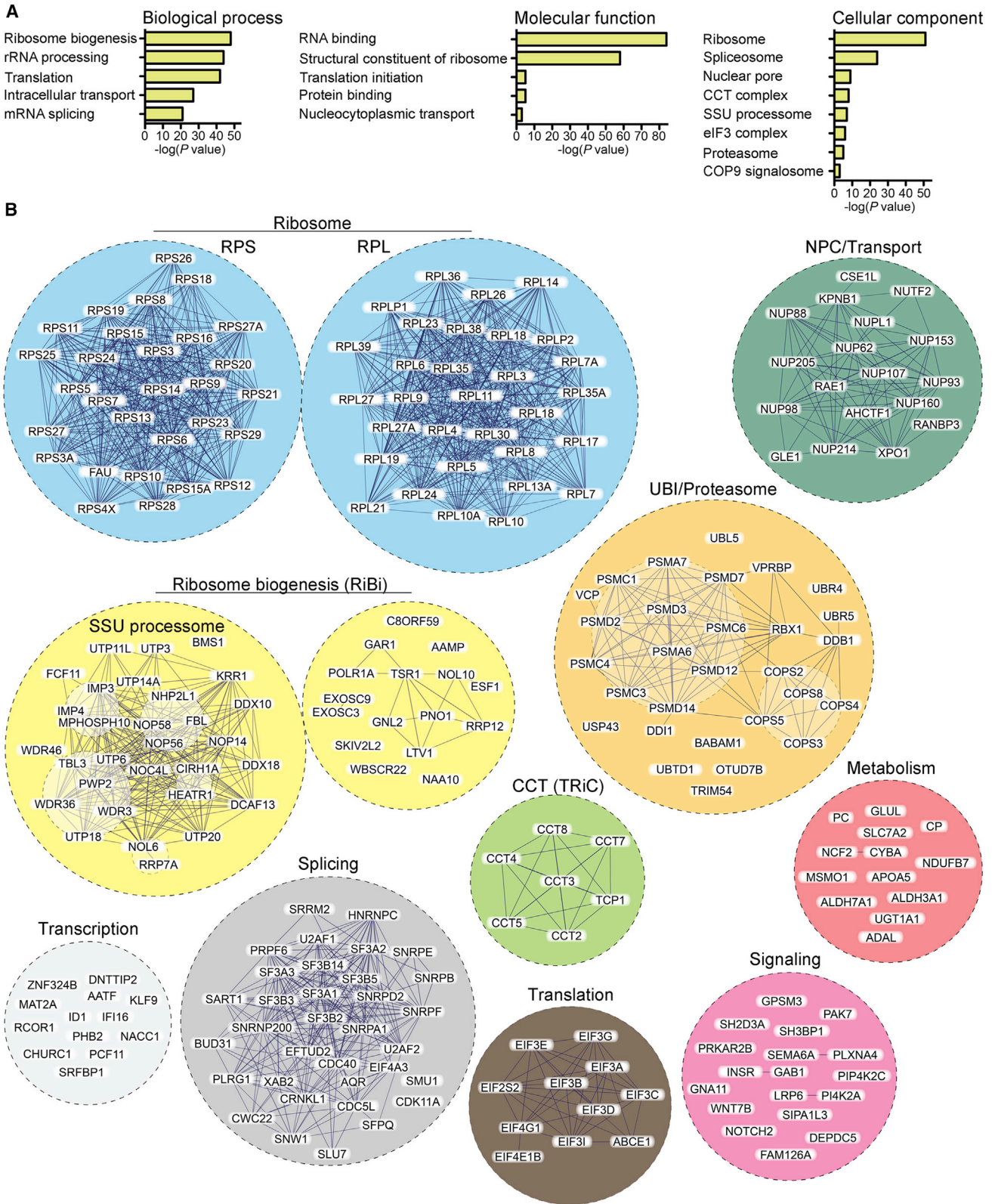
(legend on next page)

procedure. The penetrance of RPs of the 60S subunit (RPLs) reproduces our earlier findings that strong defects in 60S production affect 40S biogenesis (Wild et al., 2010).

The cluster of ribosome synthesis factors is enriched for human homologs of the yeast small subunit (SSU) processome, a large ribonucleoprotein complex composed of more than 60 factors that is required for early, nucleolar rRNA processing and 40S subunit maturation (Phipps et al., 2011). Although the physical existence of a large SSU processome-like complex remains to be proven for metazoan cells, our analysis, together with previous candidate screens (Tafforeau et al., 2013; Wild et al., 2010), provides strong evidence for a functional role of most of its predicted constituents in 40S synthesis. Consistent with an important functional role for the SSU processome in ribosome biogenesis, mutations in its components have been implicated in ribosomopathies, which are often associated with cancer susceptibility. Examples of identified disease-related SSU processome components include WDR36/UTP21, mutations of which have been suggested to result in adult-onset primary open-angle glaucoma; CIRH1A/UTP4, causing an autosomal recessive form of liver cirrhosis; and the DEAD box ATPase DDX10, a gene translocation of which induces acute myelocytic leukemia (Sondalle and Baserga, 2014).

Additional identified protein modules comprise components of the nuclear pore complex (NPC), the chaperonin-containing TCP1 complex (CCT), and splicing factors, especially subunits of the splicing factor 3 (SF3) complex. The enrichment of splicing factors may merely reflect a need for proper general pre-mRNA processing but could also be explained by effects on snoRNP biogenesis through failure to properly excise snoRNAs from introns. Interestingly, AQR/IBP160, a spliceosomal intron binding protein that couples box C/D snoRNA processing with pre-mRNA splicing (Hirose et al., 2006), ranks high on our hit list (rank 116). In the protein translation module, it is intriguing that constituents of the eIF3 translation initiation complex are strongly overrepresented, suggesting a decisive function of eIF3 for 40S subunit synthesis. Another prominent group of hits contains factors of the ubiquitin-proteasome system (UPS) and was selected for follow-up analysis (see below).

Importantly, we also identified factors involved in signaling, transcription, and metabolism that might represent part of the proteome dedicated to the control of ribosome synthesis in response to growth factor and nutrient availability. These factors and those ~18% of all hit genes that could not be assigned to any obvious functional class ("miscellaneous" category; Table S6) will be a rich source for researchers who wish to decipher the mechanistic links between diverse cellular processes and ribosome synthesis.

RBIS: A Vertebrate-Specific Ribosome Synthesis Factor

Our first follow-up analysis focused on the gene product of C8ORF59, the uncharacterized open reading frame (ORF)

ranking the highest on our list (rank 88), and was used to demonstrate that our screen identified bona fide *trans*-acting factors in ribosome biogenesis. C8ORF59 encodes a small, vertebrate-specific protein of 100 amino acids (Figure 3A) that we dubbed RBIS. Phenotypic analysis showed that RBIS depletion primarily caused a nucleoplasmic accumulation of the RPS2-YFP reporter, also reflected by a low nucleolar accumulation score of 0.24 (Table S5).

Analysis of RBIS localization revealed that RBIS is a nuclear protein that is strongly enriched in nucleoli (Figure 3B; Figure S2). To determine whether RBIS is required for nucleolar pre-rRNA synthesis, we performed fluorescence in situ hybridization (FISH) experiments using a 5′ ETS1 probe detecting the initial 47S rRNA precursor (Figure 3C). Whereas, as expected, depletion of the catalytic subunit of Pol I [si-POLR1A] strongly reduced the levels of early, nucleolar pre-rRNAs (Figure 3D; Figure S2C), downregulation of RBIS did not, suggesting that RBIS functions downstream of transcription. Northern blot analysis of rRNA from cells depleted of RBIS revealed a weak accumulation of 41S and 21S rRNA but no major defects in rRNA processing (Figure S2D). Quantification of pulse-labeling experiments following pre-rRNA maturation showed that depletion of RBIS reduced the levels of both mature 18S and 28S rRNA relative to 47/45S pre-rRNA, indicating that RBIS is required for efficient 40S and 60S subunit production (Figures 3E and 3F).

To confirm this observation, we analyzed the effect of RBIS depletion on 40S and 60S subunit synthesis using RPS2-YFP and RPL29-GFP reporter cells (Wild et al., 2010). Downregulation of RBIS indeed impaired 40S and 60S subunit biogenesis, as revealed by nuclear accumulation of both ribosomal reporter proteins as well as by nucleoplasmic accumulation of endogenous ENP1/BYSTIN and MRTO4, two *trans*-acting factors involved in maturation of the small and large subunit, respectively (Figures 3G and 3H; Figure S2E). Relocalization of ENP1 and MRTO4 to the nucleoplasm could be rescued using an siRNA targeting the 3′ UTR of the RBIS mRNA combined with ectopic expression of RBIS, excluding possible off-target effects (Figure S2F). Notably, RBIS depletion also induced nucleoplasmic accumulation of RIOK2 (Figure S2G), a protein kinase known to support cytoplasmic remodeling and nuclear export of pre-40S subunits (Zemp et al., 2009). RIOK2 is cytoplasmic at steady state and harbors a leucine-rich nuclear export signal recognized by the exportin XPO1 (Zemp et al., 2009). Nuclear accumulation of RIOK2 upon RBIS depletion was, however, not merely the result of a general defect in XPO1-mediated protein export (Figure S2G). Therefore, the observed nucleoplasmic accumulation of *trans*-acting factors and fluorescent ribosomal reporter proteins is indicative of a key role for RBIS in nucleoplasmic maturation or export of ribosomal subunits.

To test whether RBIS is a *trans*-acting factor in ribosome biogenesis, we analyzed whether RBIS is associated with pre-40S or pre-60S pre-ribosomal particles isolated by tandem

---

Figure 2. Functional Classification of Factors that Support 40S Maturation Steps
(A) GO term analysis for the group of 302 hit genes (Table S5) with respect to "biological process," "molecular function," and "cellular component" (p < 0.05).
(B) Classification of identified factors into functional clusters. Connections between genes within a cluster indicate high-confidence (>0.7) STRING interactions. Subclusters are highlighted by white circles. Genes assigned to the miscellaneous category (Table S6) are not shown.
See also Figure S1 and Tables S5, S6, S7, and S8.

Figure 3. RBIS Is a *trans*-Acting Ribosome Biogenesis Factor Specific for Vertebrates

(A) Multiple-sequence alignment of RBIS homologs from vertebrate species.

(B) HeLa K cells were analyzed by immunofluorescence (IF) of RBIS and the nucleolar marker MRTO4.

(C) Schematic of the major pre-rRNA processing steps in human cells, indicating the rRNA regions detected by probes used for FISH and northern blotting experiments.

(legend continued on next page)

affinity purifications (TAPs) using the *trans*-acting factors LTV1 and MRTO4 as baits (Wild et al., 2010; Wyler et al., 2011). Surprisingly, RBIS could only be identified as part of pre-60S particles isolated by MRTO4-TAP, like RLP24 and NMD3, two well characterized, 60S-specific *trans*-acting factors (Saveanu et al., 2003; Thomas and Kutay, 2003; Trotta et al., 2003), but was absent from pre-40S particles retrieved by TAP-LTV1 (Figure 3I). Consistent with a role of RBIS in 60S subunit synthesis, polysome profiling by sucrose gradient analysis revealed the appearance of half-mer polysomes upon RBIS depletion, indicative of a 60S subunit shortage (Figure 3J).

Collectively, our analysis identifies RBIS as a vertebrate-specific *trans*-acting factor in ribosome biogenesis. Because RBIS resembles RPs in both its small size and basic isoelectric point, it could potentially chaperone rRNA during maturation or act as placeholder for a ribosomal protein. At least two different scenarios might explain the observed defects in maturation of both ribosomal subunits upon RBIS depletion despite the selective interaction of RBIS with pre-60S particles: RBIS acts at a nucleolar step of ribosome biogenesis that affects the fate of both subunits, and, after their endonucleolytic separation, it remains selectively associated with pre-60S; or RBIS is a 60S-specific *trans*-acting factor, and the 60S biogenesis defect caused by its depletion indirectly affects the production of 40S subunits (Wild et al., 2010). Because the presence of RBIS is required for biogenesis of both subunits, it may well contribute to their balanced synthesis.

The CUL4-RING E3 Ubiquitin Ligase Complex Is Required for Ribosome Synthesis

The early steps of ribosome biogenesis are known to be promptly sensitive to inhibition of the proteasome (Fátyol and Grummt, 2008; Lam et al., 2007; Stavreva et al., 2006), a multi-protein complex responsible for the degradation of polyubiquitinated proteins. Thus, the activity of the cell's major protein degradation complex sustains the ability of cells to produce new ribosomes for protein synthesis. However, how protein degradation is linked to ribosome synthesis has remained elusive. Therefore, we focused our second follow-up on the UPS cluster and exploited the predictive power of our dataset to identify key players in this pathway. In the UPS module, we not only detected several proteasome subunits but also the COP9 signalosome (CSN), a regulator of cullin-RING E3 ligases (CRLs) (Figure 2B). CRLs represent the largest class of ubiquitin ligases and consist of scaffolding cullins and characteristic sets

of associated factors (Petroski and Deshaies, 2005). Strikingly, not only RBX1 (rank 203), a ring finger protein shared between most CRLs, but also the linker protein DDB1 (rank 78), specific to CUL4 E3 ubiquitin ligase (CRL4) complexes, caused nucleolar accumulation of RPS2-YFP (Figure S3A; Table S5), suggesting a role of CRL4 in 40S production.

In humans, two genes encode for CUL4 (CUL4A and CUL4B), and they share extensive homology and functional redundancy (Jackson and Xiong, 2009; Sharma and Nag, 2014), potentially explaining why CUL4 itself was not identified in our screen. Interestingly, both CUL4 proteins have been detected in purified nucleoli (Ahmad et al., 2009). To investigate whether CRL4 is required for 40S subunit synthesis, as predicted by our screening data, we analyzed the effect of the downregulation of CUL4A and CUL4B on 40S subunit synthesis using the RPS2-YFP reporter. Although individual depletion of either CUL4A or CUL4B had only a very mild effect on 40S synthesis, their combined downregulation caused a nucle(ol)ar accumulation of the reporter protein (Figure S3B).

To substantiate this observation, we used changes in the dynamic localization of the 40S *trans*-acting factor ENP1 as an assay. Under steady-state conditions, ENP1 predominantly localizes to nucleoli, from where it shuttles, along with newly synthesized 40S subunits, into the cytoplasm. When nuclear export of pre-40S is inhibited by leptomycin B (LMB), which blocks XPO1-mediated 40S subunit export, ENP1 accumulates in the nucleoplasm as part of 40S precursors (Figure 4A). This nucleoplasmic accumulation of ENP1 is prevented by early biogenesis defects that trap pre-40S subunits in nucleoli; e.g., by depletion of FBL. Similarly, co-depletion of CUL4A and CUL4B resulted in a failure of ENP1 release from nucleoli, indicative for a defect in nucleolar 40S biogenesis steps (Figure 4A). The same phenotype was observed upon downregulation of DDB1 and RBX1. Also, depletion of selected subunits of the CSN and the proteasome reproduced this defect, underscoring the involvement of the UPS in 40S subunit synthesis (Figures 4A; Figure S3C). Notably, although depletion of POLR1A, which reduces rRNA transcription, was accompanied by a reduction of nucleolar size, depletion of CUL4A/B, DDB1, RBX1, CSN, and proteasome subunits was not, suggesting a function of these factors downstream of transcription. rRNA pulse-labeling analysis revealed a reduction of newly synthesized mature 18S and 28S rRNA relative to 47/45S pre-rRNA upon CUL4A/B co-depletion and DDB1 RNAi, indicating that the CRL4-DDB1 complex assists with the production of both the 40S and 60S subunits (Figures 4B and 4C). Taken

(D) HeLa K cells were treated with the indicated siRNAs, fixed, and analyzed by FISH with a 5′ ETS1 probe. Ctrl, control.

(E) HeLa K cells were treated with the indicated siRNAs, followed by pulse-labeling with ^{33}P-orthophosphate. Total RNA was separated by gel electrophoresis, and pre-rRNA processing was analyzed by autoradiography.

(F) Quantification of the experiment in (E) (at t = 240 min). Data are mean ± SEM from three experiments. *$p \leq 0.05$, **$p \leq 0.01$, ***$p \leq 0.001$ (one-way ANOVA and Dunnett's test).

(G) Tetracycline-inducible reporter cells were transfected with the indicated siRNAs. 52 hr post-RNAi, RPS2-YFP cells were induced for 16 hr, followed by a 4-hr chase in tetracycline-free medium. RPL29-GFP cells were induced 44 hr post-RNAi for 8 hr, followed by a 20-hr chase. Both cell lines were fixed 72 hr after siRNA transfection and analyzed by confocal microscopy.
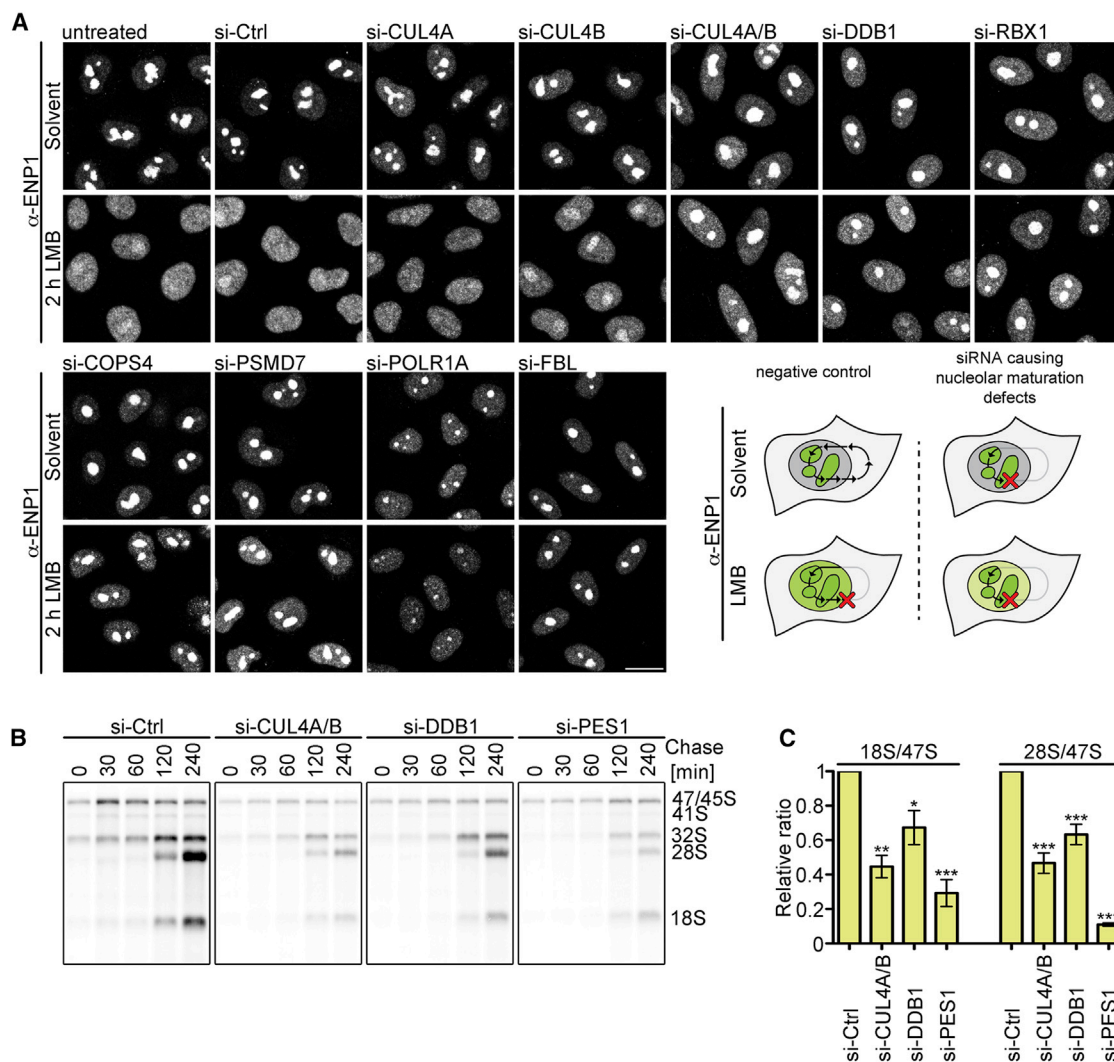
(H) HeLa K cells were treated with the indicated siRNAs, fixed, and analyzed by IF of ENP1 (40S) and MRTO4 (60S).

(I) Pre-ribosomal particles were purified from HEK293 cells bearing an inducible copy of TAP-tagged MRTO4 (60S) or LTV1 (40S) after 24 hr of tetracycline induction, followed by western blot analysis. TAP-GFP served as a negative control.

(J) HeLa K cells were treated with the indicated siRNAs, followed by sucrose gradient centrifugation of cell extracts and polysome profiling.

Scale bars, 20 μm. See also Figure S2.

Figure 4. CUL4-RING E3 Ubiquitin Ligase Complexes Contribute to the Synthesis of Ribosomes

(A) HeLa K cells were transfected with the indicated siRNAs. After 72 hr, cells were subjected either to a solvent control or treated with 20 nM LMB for 2 hr, followed by fixation and IF analysis of ENP1. Also shown is a schematic of the experiment. Under control conditions, ENP1 shuttles between the nucleolus and the cytoplasm as a constituent of maturing 40S subunits but is nucleolar at steady state. If 40S subunit export is inhibited by LMB treatment, then ENP1 accumulates in the nucleoplasm (Zemp et al., 2009). Depletion of factors required for nucleolar maturation of pre-40S subunits can lead to a failure of release of pre-40S from nucleoli, manifested by diminished nucleoplasmic ENP1 in the presence of LMB. Scale bar, 20 μm.

(B) HeLa K cells were transfected with the indicated siRNAs, and pre-rRNA maturation was analyzed by pulse-labeling as shown in Figure 3E.

(C) Quantification of the experiment shown in (B) (240-min chase) as shown in Figure 3F.

See also Figure S3.

together, as predicted by the presence of the proteasome, the COP9 signalosome, RBX1, and DDB1 in the results of our screen, CUL4A/B function is also required for ribosome biogenesis.

Previous studies have demonstrated that RPs are produced in excess and that unassembled RPs are degraded continuously (Lam et al., 2007), perhaps to prevent potential dominant-negative effects on ribosome assembly. However, the responsible ubiquitin ligases have remained elusive. Our data identify CRL4 as a candidate E3 ligase for this process based on the similar effects of proteasome inhibition and CRL4 depletion on ribosome synthesis. It is also possible that CRL4 assists with ribosome synthesis by different means, for instance by ubiquitination of RiBi factors (Matsumoto et al., 2005; Peng et al., 2003) or through its role in chromatin regulation (Jackson and Xiong, 2009; Sharma and Nag, 2014). Because CUL4 has been described as an attractive target for therapeutic interventions in cancer and other human diseases (Sharma and Nag, 2014), it will be all the more important to understand the molecular mechanisms accounting for the observed ribosome biogenesis defects. The identification of CRL4 as a novel regulator of ribosome biogenesis guides the way for this endeavor. Toward this goal, it will be essential to identify the respective ubiquitination substrates

of CLR4. Substrate specificity of CRL4 is determined by a set of DDB1- and CUL4-associated factors (DCAFs) (Lee and Zhou, 2007). Among the hits in our screen, there are a number of proven or putative substrate-specific adaptors of CRL4, like DCAF1/VPRBP (rank 33), a promiscuous substrate adaptor (Nakagawa et al., 2013), or DCAF13/WDSOF1 (rank 38), a potential SSU component (Phipps et al., 2011), again emphasizing the predictive strength of our dataset.

The Glutamine Synthetase GLUL Supports Ribosome Biogenesis

Among the identified metabolic enzymes was GLUL (rank 266). GLUL catalyzes intracellular production of L-glutamine (Gln) by ATP-dependent addition of ammonia to glutamate. For many cancer cells, Gln is a central nutrient, providing carbon and nitrogen for protein and nucleotide synthesis, whereas its conversion into α-ketoglutarate fuels ATP production (Lunt and Vander Heiden, 2011; Wise and Thompson, 2010). Because GLUL opposes the metabolic flux in this direction, its identification in our screen was unpredicted. Depletion of GLUL by RNAi resulted in a prominent 40S biogenesis defect, reflected by nucleoplasmic accumulation of RPS2-YFP in reporter cells and of the 40S trans-acting factors ENP1, RRP12, DIM2, and NOB1 in HeLa K cells (Figures 5A–5C). In contrast, production of 60S subunits, inspected by RPL29-GFP and eIF6 localization, was only affected weakly.

A major cellular hub integrating the availability of amino acids, including Gln, is the mTOR kinase signaling pathway (Shimobayashi and Hall, 2014). In humans, two distinct mTOR protein complexes exist, specified by the mTOR kinase-associated factors RAPTOR (mTORC1) and RICTOR (mTORC2) (Laplante and Sabatini, 2012). mTORC1 is known to regulate ribosome biogenesis at various levels (Gentilella et al., 2015). To elucidate whether GLUL depletion influences mTORC1 activity and, thereby, 40S subunit biogenesis, we compared the effect of GLUL and RAPTOR depletion. As expected, depletion of RAPTOR caused an early ribosome biogenesis defect (Figure S4B), manifesting in a failure of ENP1 to accumulate in the nucleoplasm in the presence of LMB. In contrast, GLUL depletion led to nucleoplasmic accumulation of ENP1 in the absence of LMB. Furthermore, there was no obvious defect in mTORC1 signaling upon GLUL depletion, indicated by the efficient phosphorylation of the mTORC1 downstream targets 4EBP1 and RPS6 (Figure S4C). We conclude that GLUL influences 40S synthesis by an mTORC1-independent mechanism. Interestingly, we observed that depletion of RICTOR induced nucleoplasmic accumulation of ENP1 (Figure S4B), revealing an unexpected contribution of mTORC2 to the maturation of ribosomal subunits.

In proliferating cells, the majority of total transcription is dedicated to rRNA production (Warner, 1999). Because Gln is an obligate nitrogen donor for various steps of purine and pyrimidine synthesis (Wise and Thompson, 2010), we investigated rRNA transcription in cells depleted of GLUL. Surprisingly, analysis of 47S rRNA levels by FISH (Figure 5D) and pulse-labeling analysis (Figures 5E and 5F) revealed no reduction in rRNA transcription, suggesting that the effect of GLUL depletion on 40S subunit synthesis is downstream of transcription. Furthermore, measurements of the abundance of multiple nucleotides and their

precursors by flow injection time of flight (TOF) mass spectrometry (MS) showed no significant concentration changes (Figures S4D and S4E), indicating that nucleotides are not limiting for rRNA synthesis in cells depleted of GLUL. In contrast, GLUL depletion led to rRNA processing defects, illustrated by an increased 5′ ITS1 signal in FISH experiments (Figure 5D, bottom), a pile-up of precursors to 18S rRNA observed by northern blotting, and a reduction of newly synthesized 18S and 28S rRNAs relative to 47/45S pre-rRNA (Figures 5G–5I).

As ribosome biogenesis is a highly energy-consuming process (Warner, 1999), we analyzed the levels of various energy-rich carrier molecules after GLUL depletion. However, neither the level of NADH, a reducing agent derived from the tricarboxylic acid (TCA) cycle, nor total ATP or guanosine triphosphate (GTP) levels appeared to be changed (Figure S4E), suggesting that the observed ribosome biogenesis defect cannot be explained by an overall lack of energy in GLUL-depleted cells. Consistently, there was also no reduction in global translation upon downregulation of GLUL compared with cells treated with control siRNAs (Figures S4F and S4G). Although general protein synthesis remained unperturbed upon depletion of GLUL, it cannot be completely excluded that synthesis of certain Gln-rich proteins is diminished.

Our RNAi experiments were performed in complete medium containing Gln, which is known to be unstable. We reasoned that reduced uptake of Gln, because of limiting extracellular levels over the time course of the experiment, may render ribosome synthesis sensitive to inactivation of GLUL. Indeed, adding 10 mM Gln to the medium at regular intervals of 12 hr attenuated the ribosome biogenesis defects (Figures 6A and 6B). However, to restore the production of ribosomes, a high dose of Gln was required (data not shown), exceeding the standard concentration in cell culture media 5-fold. These data show that a high concentration of extracellular glutamine can overcome the lack of intracellular Gln synthesis in HeLa cells.

Consequently, we tested whether there is a direct connection between intracellular Gln synthesis by GLUL (i.e., its enzymatic activity) and the capability of GLUL to support ribosome biogenesis. GLUL expression was downregulated by an siRNA targeting the 3′ UTR of the GLUL mRNA, resulting in the expected accumulation of ENP1 in the nucleoplasm. Expression of wild-type GLUL rescued 40S biogenesis and restored the predominantly nucleolar localization of ENP1 (Figure 6C). Strikingly, expression of GLUL variants impaired in synthetase activity by mutation of Arg324 (R324A or R324C), a strictly conserved residue situated in the substrate-binding pocket of GLUL and involved in ATP binding (Krajewski et al., 2008), did not rescue the 40S biogenesis defect. It is noteworthy that congenital mutations of R324 in human GLUL cause defects in brain development and neonatal death (Häberle et al., 2005), highlighting the importance of intracellular Gln synthesis for tissue homeostasis and development.

These data show that the catalytic activity of GLUL is central to 40S production in HeLa cells. Interestingly, maturation of 40S subunits appears to react to failure in intracellular Gln synthesis before significant changes in other intracellular metabolites can be detected. A previous study has revealed that depletion of extracellular Gln synergizes with increased MYC expression in driving apoptosis of cancer cells (Yuneva et al., 2007). In this
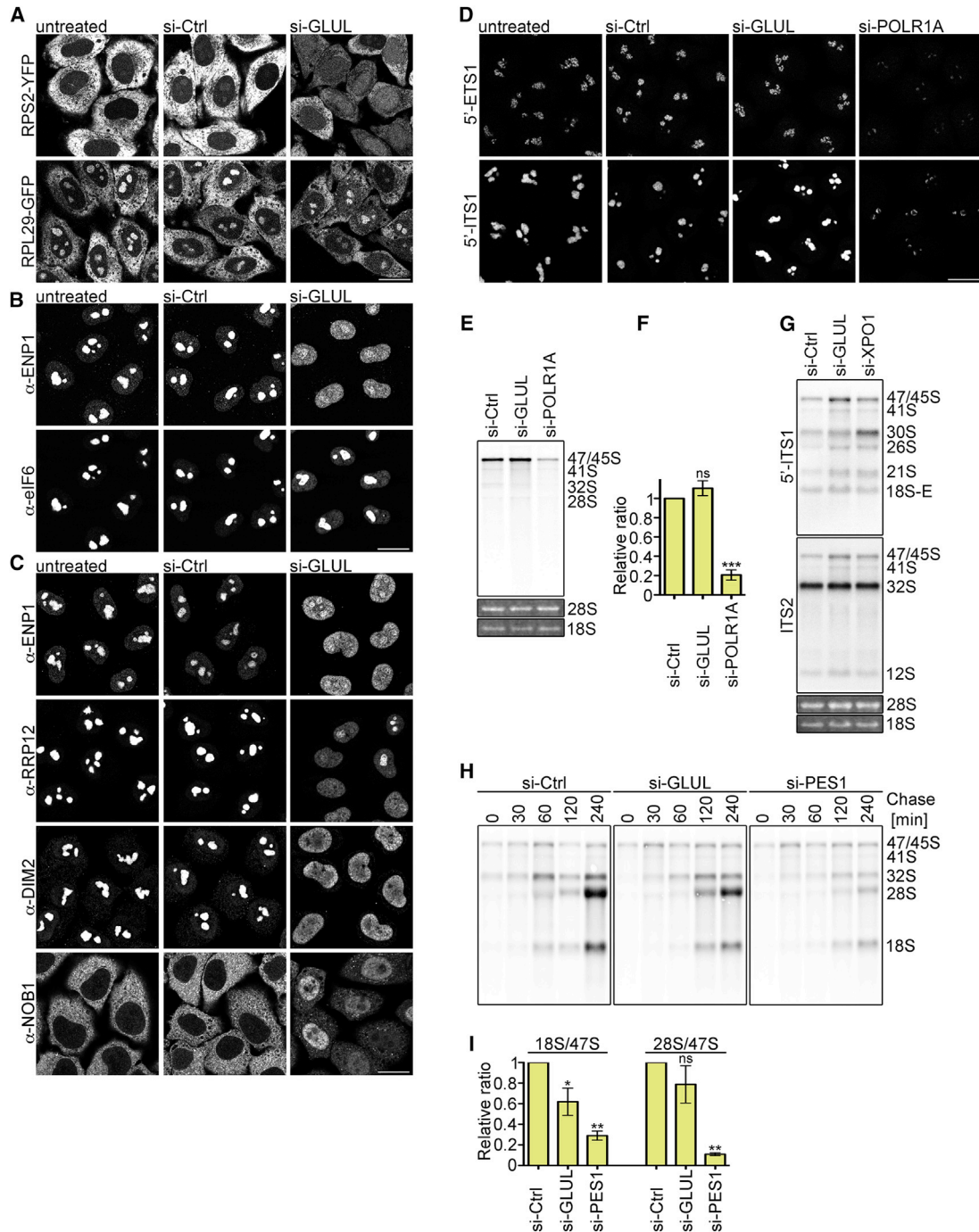
Figure 5. GLUL Supports the Production of Ribosomal Subunits in HeLa Cells

(A) Tetracycline-inducible reporter cells were transfected with the indicated siRNAs and analyzed as described in Figure 3G.

(B) HeLa K cells treated with the indicated siRNAs were analyzed by IF of ENP1 (40S) and eIF6 (60S).

(C) Experiment as in (B). Shown is the IF analysis of the 40S *trans*-acting factors ENP1, RRP12, DIM2, and NOB1.

(D) HeLa K cells were transfected with the indicated siRNAs, and localization of pre-rRNA was analyzed by FISH using the 5′ ETS1 or 5′ ITS1 probes.

(E) HeLa K cells were treated with the indicated siRNAs, pulse-labeled with ^{33}P for 30 min, and analyzed as shown in Figure 3E.

(F) 47/45S pre-rRNA levels from (E) were analyzed as in Figure 3F. ***p $\leq$ 0.001; ns, not significant.

(G) Northern blot analysis of RNA isolated from cells treated with the indicated siRNAs using probes directed to the 5′ ITS1 or ITS2 (Figure 3C).

(H) After treatment of HeLa K cells with the indicated siRNAs, pre-rRNA maturation was followed by pulse-labeling as shown in Figure 3E.

(I) Quantification of the experiment shown in (H) (240-min chase) as in Figure 3F. *p $\leq$ 0.05, **p $\leq$ 0.01.

Scale bars, 20 μm. See also Figure S4.
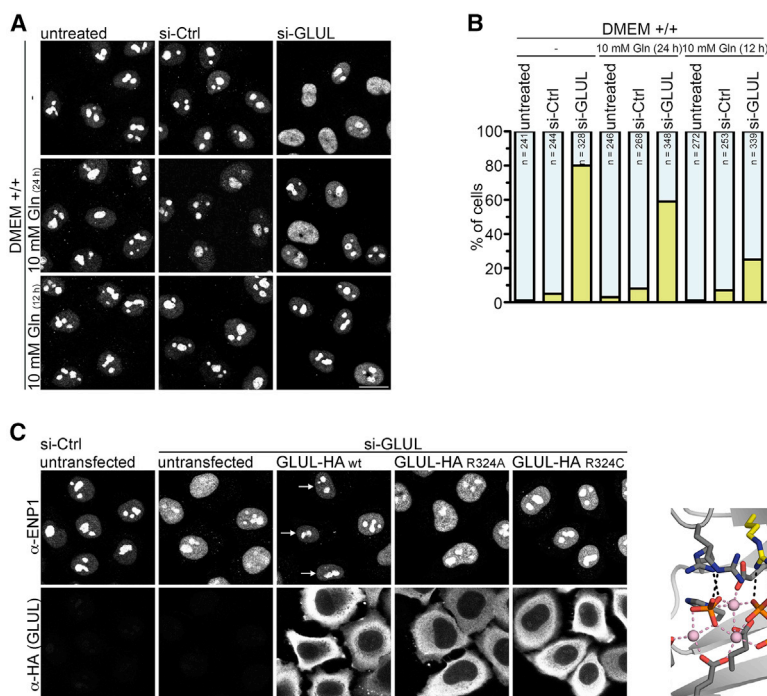
Figure 6. The Catalytic Activity of GLUL Is Required for the Efficient Synthesis of 40S Subunits

(A) HeLa K cells were subjected to RNAi for 72 hr. In the course of the experiment, the cell culture medium was supplemented with 10 mM fresh Gln every 24 or 12 hr.

(B) Quantification of the experiment shown in (A). n, number of counted cells.

(C) HeLa K cells were transfected with Ctrl siRNA or an siRNA targeting the 3′ UTR of the GLUL mRNA. 24 hr post-transfection, cells were transiently transfected with different HA-tagged GLUL constructs. Cells were fixed after another 48 hr and analyzed by IF of ENP1 and HA (GLUL). GLUL-HA-expressing cells, marked by white arrowheads, are insensitive to depletion of endogenous GLUL. Depiction of the glutamate-binding pocket of GLUL (PDB ID code 2OJW) generated by PyMOL. Arg324 (yellow) is involved in binding of ATP (phosphates shown in orange) and, therefore, crucial for the catalytic activity of GLUL.

Scale bars, 20 μm. See also Figure S4.

system, similar to our studies, cellular ATP levels were not majorly affected by Gln deficiency, indicating that the cause of cell death was unrelated to energy depletion. Because MYC is a driver of ribosome biogenesis in cancer cells, it is conceivable that upregulation of ribosome synthesis renders cancer cells especially sensitive to depletion of Gln. Our data highlight that intracellular Gln synthesis is a major pillar for sustained production of 40S ribosomal subunits in HeLa cells. Although most studies have emphasized the importance of Gln as fuel for the TCA cycle (Lunt and Vander Heiden, 2011; Wise and Thompson, 2010), our data shed new light on the importance of Gln, demonstrating that cytoplasmic Gln synthesis is required for efficient ribosome synthesis. It will be interesting to decipher whether the dependency of ribosome production on GLUL activity is universal or specific to cancer cells.

Collectively, our screening results provide a rich source for studies of ribosome biogenesis and its connection to other cellular pathways. Unbalanced ribosome synthesis is the cause of devastating inherited diseases and is associated with the development of cancers. Given the complex networks of factors that assist with and control ribosome production, as highlighted by our screening data, one can expect that more disease-causing mutations in genes encoding for ribosome synthesis factors might be discovered, as exemplified by our studies on GLUL. These factors may provide a suite of promising targets for the development of new therapies affecting ribosome synthesis to treat cancer.

EXPERIMENTAL PROCEDURES

Cell Lines and Antibodies

The HeLa reporter cell line carrying a tetracycline-inducible RPS2-YFP gene has been described previously (Wild et al., 2010; Zemp et al., 2009). Analogous

RPS2-YFP or RPL29-GFP reporter cell lines for follow-up analyses were generated using a different parental HeLa Flp-In T-REx cell line (Häfner et al., 2014). HeLa K and RPE2 cells were obtained from D. Gerlich (Institute of Molecular Biotechnology) and U2OS and HaCaT cells from C. Azzalin and S. Werner (ETH Zurich), respectively. All cell lines were grown in DMEM supplemented with 10% fetal calf serum (FCS) and 1× penicillin/streptomycin (DMEM+/+) at 37°C in 5% CO_2.

Antibodies against the following human proteins have been described previously: ENP1, NMD3, DIM2, NOB1, and RIOK2 (Zemp et al., 2009); RPL23A and RLP24 (Wild et al., 2010); TRS1 (Zemp et al., 2014); and RRP12 (Wyler et al., 2011). Antibodies against human RBIS were raised in rabbits against recombinant His-tagged RBIS and a C-terminal peptide (C-HESKPVNV DEATRLMALL). For commercial antibodies, see the Supplemental Experimental Procedures.

siRNA Screening Procedure

Screens were performed in 384-well plates using reverse transfection. Per well, 1 pmol siRNA dissolved in 5 μl H_2O was supplemented with transfection reagent (0.0625 μl Oligofectamine [Invitrogen] in 10 μl Opti-MEM [Life Technologies] for the primary screen and 0.125 μl INTERFERin [Polyplus transfection] in 10 μl Opti-MEM for validation screens). Plates were incubated for 30 min at room temperature (RT). Then 60 μl of HeLa RPS2-YFP cells (8,000 cells/ml in DMEM+/+) were added. Plates were incubated for 58 hr. Expression of the RPS2-YFP reporter was induced for 14 hr by addition of 10 μl DMEM+/+ supplemented with tetracycline (final concentration, 125 ng/ml). Cells were fixed by addition of 20 μl 16% paraformaldehyde (PFA) in PBS. After 10 min, cells were washed once with PBS, incubated with Hoechst in PBS for 10 min, washed again, and kept in H_2O/NaN_3. Pictures were taken by automated microscopy (MD IXM).

Access to Screening Data

Images and numerical data can be found at http://www.ribosomebiogenesis.org.

RNAi and Transient Transfections

DNA plasmids were transfected using X-tremeGENE. Transfection of siRNAs was performed with INTERFERin or RNAiMAX. The siRNAs were used at

9 nM for 72 hr unless indicated otherwise. Sequences of siRNAs and additional information are specified in the Supplemental Experimental Procedures.

Immunofluorescence

Cells were fixed in 4% PFA and permeabilized in 0.1% Triton X-100, 0.02% SDS in PBS for 5 min. All subsequent steps were performed as described previously (Zemp et al., 2009).

FISH

FISH was carried out as described previously (Rouquette et al., 2005) using 5′ Cy5-labeled probes targeting the 5′ ETS1 (Granneman et al., 2004), ETS1, or 5′ ITS1 (Rouquette et al., 2005).

rRNA Pulse-Labeling

Cells were starved in phosphate-free DMEM (Invitrogen) for 1 hr at 37°C followed by pulse-labeling in phosphate-free DMEM supplemented with ^{33}P-phosphoric acid (20 μCi/ml) for 1 hr at 37°C. The cells were washed with DMEM+/+, and, after different chase periods in nonradioactive DMEM+/+, total RNA was extracted using the RNeasy mini kit (QIAGEN). RNA derived from an equal number of cells was separated on a 1.2% agarose gel in 50 mM HEPES (pH 7.8) and 6% formaldehyde and transferred to a nylon membrane by capillary transfer. The membrane was analyzed by phospho-imaging.

TAP

Purification of pre-ribosomal particles was performed as described previously (Wyler et al., 2011).

SUPPLEMENTAL INFORMATION

Supplemental Information includes Supplemental Experimental Procedures, four figures, and eight tables and can be found with this article online at http://dx.doi.org/10.1016/j.celrep.2015.11.061.

AUTHOR CONTRIBUTIONS

ACKNOWLEDGMENTS

REFERENCES

Ahmad, Y., Boisvert, F.-M., Gregor, P., Cobley, A., and Lamond, A.I. (2009). NOPdb: Nucleolar Proteome Database–2008 update. Nucleic Acids Res. 37, D181–D184.

Andersen, J.S., Lam, Y.W., Leung, A.K., Ong, S.E., Lyon, C.E., Lamond, A.I., and Mann, M. (2005). Nucleolar proteome dynamics. Nature 433, 77–83.

Bywater, M.J., Pearson, R.B., McArthur, G.A., and Hannan, R.D. (2013). Dysregulation of the basal RNA polymerase transcription apparatus in cancer. Nat. Rev. Cancer 13, 299–314.

Carpenter, A.E., Jones, T.R., Lamprecht, M.R., Clarke, C., Kang, I.H., Friman, O., Guertin, D.A., Chang, J.H., Lindquist, R.A., Moffat, J., et al. (2006). CellProfiler: image analysis software for identifying and quantifying cell phenotypes. Genome Biol. 7, R100.

Deisenroth, C., and Zhang, Y. (2010). Ribosome biogenesis surveillance: probing the ribosomal protein-Mdm2-p53 pathway. Oncogene 29, 4253–4260.

Drygin, D., Rice, W.G., and Grummt, I. (2010). The RNA polymerase I transcription machinery: an emerging target for the treatment of cancer. Annu. Rev. Pharmacol. Toxicol. 50, 131–156.

Fátyol, K., and Grummt, I. (2008). Proteasomal ATPases are associated with rDNA: the ubiquitin proteasome system plays a direct role in RNA polymerase I transcription. Biochim. Biophys. Acta 1779, 850–859.

Franceschini, A., Szklarczyk, D., Frankild, S., Kuhn, M., Simonovic, M., Roth, A., Lin, J., Minguez, P., Bork, P., von Mering, C., and Jensen, L.J. (2013). STRING v9.1: protein-protein interaction networks, with increased coverage and integration. Nucleic Acids Res. 41, D808–D815.

Gentilella, A., Kozma, S.C., and Thomas, G. (2015). A liaison between mTOR signaling, ribosome biogenesis and cancer. Biochim. Biophys. Acta 1849, 812–820.

Granneman, S., Vogelzangs, J., Lührmann, R., van Venrooij, W.J., Pruijn, G.J., and Watkins, N.J. (2004). Role of pre-rRNA base pairing and 80S complex formation in subnucleolar localization of the U3 snoRNP. Mol. Cell. Biol. 24, 8600–8610.

Häberle, J., Görg, B., Rutsch, F., Schmidt, E., Toutain, A., Benoist, J.F., Gelot, A., Suc, A.L., Höhne, W., Schliess, F., et al. (2005). Congenital glutamine deficiency with glutamine synthetase mutations. N. Engl. J. Med. 353, 1926–1933.

Häfner, J., Mayr, M.I., Möckel, M.M., and Mayer, T.U. (2014). Pre-anaphase chromosome oscillations are regulated by the antagonistic activities of Cdk1 and PP1 on Kif18A. Nat. Commun. 5, 4397.

Hannan, K.M., Sanij, E., Rothblum, L.I., Hannan, R.D., and Pearson, R.B. (2013). Dysregulation of RNA polymerase I transcription during disease. Biochim. Biophys. Acta 1829, 342–360.

Henras, A.K., Soudet, J., Gérus, M., Lebaron, S., Caizergues-Ferrer, M., Mougin, A., and Henry, Y. (2008). The post-transcriptional steps of eukaryotic ribosome biogenesis. Cell. Mol. Life Sci. 65, 2334–2359.

Hirose, T., Ideue, T., Nagai, M., Hagiwara, M., Shu, M.D., and Steitz, J.A. (2006). A spliceosomal intron binding protein, IBP160, links position-dependent assembly of intron-encoded box C/D snoRNP to pre-mRNA splicing. Mol. Cell 23, 673–684.

Jackson, S., and Xiong, Y. (2009). CRL4s: the CUL4-RING E3 ubiquitin ligases. Trends Biochem. Sci. 34, 562–570.

König, R., Chiang, C.Y., Tu, B.P., Yan, S.F., DeJesus, P.D., Romero, A., Bergauer, T., Orth, A., Krueger, U., Zhou, Y., and Chanda, S.K. (2007). A probability-based approach for the analysis of large-scale RNAi screens. Nat. Methods 4, 847–849.

Krajewski, W.W., Collins, R., Holmberg-Schiavone, L., Jones, T.A., Karlberg, T., and Mowbray, S.L. (2008). Crystal structures of mammalian glutamine synthetases illustrate substrate-induced conformational changes and provide opportunities for drug and herbicide design. J. Mol. Biol. 375, 217–228.

Lam, Y.W., Lamond, A.I., Mann, M., and Andersen, J.S. (2007). Analysis of nucleolar protein dynamics reveals the nuclear degradation of ribosomal proteins. Curr. Biol. 17, 749–760.

Laplante, M., and Sabatini, D.M. (2012). mTOR signaling in growth control and disease. Cell 149, 274–293.

Lee, J., and Zhou, P. (2007). DCAFs, the missing link of the CUL4-DDB1 ubiquitin ligase. Mol. Cell 26, 775–780.

Leung, A.K.L., Trinkle-Mulcahy, L., Lam, Y.W., Andersen, J.S., Mann, M., and Lamond, A.I. (2006). NOPdb: Nucleolar Proteome Database. Nucleic Acids Res. 34, D218–D220.

Lunt, S.Y., and Vander Heiden, M.G. (2011). Aerobic glycolysis: meeting the metabolic requirements of cell proliferation. Annu. Rev. Cell Dev. Biol. 27, 441–464.

Matsumoto, M., Hatakeyama, S., Oyamada, K., Oda, Y., Nishimura, T., and Nakayama, K.I. (2005). Large-scale analysis of the human ubiquitin-related proteome. Proteomics 5, 4145–4151.

Nagaraj, N., Wisniewski, J.R., Geiger, T., Cox, J., Kircher, M., Kelso, J., Pääbo, S., and Mann, M. (2011). Deep proteome and transcriptome mapping of a human cancer cell line. Mol. Syst. Biol. 7, 548.

Nakagawa, T., Mondal, K., and Swanson, P.C. (2013). VprBP (DCAF1): a promiscuous substrate recognition subunit that incorporates into both RING-family CRL4 and HECT-family EDD/UBR5 E3 ubiquitin ligases. BMC Mol. Biol. 14, 22.

Peng, J., Schwartz, D., Elias, J.E., Thoreen, C.C., Cheng, D., Marsischky, G., Roelofs, J., Finley, D., and Gygi, S.P. (2003). A proteomics approach to understanding protein ubiquitination. Nat. Biotechnol. 21, 921–926.

Petroski, M.D., and Deshaies, R.J. (2005). Function and regulation of cullin-RING ubiquitin ligases. Nat. Rev. Mol. Cell Biol. 6, 9–20.

Phipps, K.R., Charette, J., and Baserga, S.J. (2011). The small subunit processome in ribosome biogenesis—progress and prospects. Wiley Interdiscip. Rev. RNA 2, 1–21.

Reimand, J., Arak, T., and Vilo, J. (2011). g:Profiler–a web server for functional interpretation of gene lists (2011 update). Nucleic Acids Res. 39, W307–W315.

Rouquette, J., Choesmel, V., and Gleizes, P.E. (2005). Nuclear export and cytoplasmic processing of precursors to the 40S ribosomal subunits in mammalian cells. EMBO J. 24, 2862–2872.

Saveanu, C., Namane, A., Gleizes, P.E., Lebreton, A., Rousselle, J.C., Noaillac-Depeyre, J., Gas, N., Jacquier, A., and Fromont-Racine, M. (2003). Sequential protein association with nascent 60S ribosomal particles. Mol. Cell. Biol. 23, 4449–4460.

Schaab, C., Geiger, T., Stoehr, G., Cox, J., and Mann, M. (2012). Analysis of high accuracy, quantitative proteomics data in the MaxQB database. Mol. Cell. Proteomics 11, 014068.

Sharma, P., and Nag, A. (2014). CUL4A ubiquitin ligase: a promising drug target for cancer and other human diseases. Open Biol. 4, 130217.

Shimobayashi, M., and Hall, M.N. (2014). Making new contacts: the mTOR network in metabolism and signalling crosstalk. Nat. Rev. Mol. Cell Biol. 15, 155–162.

Sondalle, S.B., and Baserga, S.J. (2014). Human diseases of the SSU processome. Biochim. Biophys. Acta 1842, 758–764.

Stavreva, D.A., Kawasaki, M., Dundr, M., Koberna, K., Müller, W.G., Tsujimura-Takahashi, T., Komatsu, W., Hayano, T., Isobe, T., Raska, I., et al. (2006). Potential roles for ubiquitin and the proteasome during ribosome biogenesis. Mol. Cell. Biol. 26, 5131–5145.

Stumpf, C.R., and Ruggero, D. (2011). The cancerous translation apparatus. Curr. Opin. Genet. Dev. 21, 474–483.

Tafforeau, L., Zorbas, C., Langhendries, J.-L., Mullineux, S.-T., Stamatopoulou, V., Mullier, R., Wacheul, L., and Lafontaine, D.L.J. (2013). The complexity of human ribosome biogenesis revealed by systematic nucleolar screening of Pre-rRNA processing factors. Mol. Cell 51, 539–551.

Teng, T., Thomas, G., and Mercer, C.A. (2013). Growth control and ribosomopathies. Curr. Opin. Genet. Dev. 23, 63–71.

Thomas, F., and Kutay, U. (2003). Biogenesis and nuclear export of ribosomal subunits in higher eukaryotes depend on the CRM1 export pathway. J. Cell Sci. 116, 2409–2419.

Thomson, E., Ferreira-Cerca, S., and Hurt, E. (2013). Eukaryotic ribosome biogenesis at a glance. J. Cell Sci. 126, 4815–4821.

Trotta, C.R., Lund, E., Kahan, L., Johnson, A.W., and Dahlberg, J.E. (2003). Coordinated nuclear export of 60S ribosomal subunits and NMD3 in vertebrates. EMBO J. 22, 2841–2851.

Tschochner, H., and Hurt, E. (2003). Pre-ribosomes on the road from the nucleolus to the cytoplasm. Trends Cell Biol. 13, 255–263.

Turowski, T.W., and Tollervey, D. (2015). Cotranscriptional events in eukaryotic ribosome synthesis. Wiley Interdiscip. Rev. RNA 6, 129–139.

Warner, J.R. (1999). The economics of ribosome biosynthesis in yeast. Trends Biochem. Sci. 24, 437–440.

Wild, T., Horvath, P., Wyler, E., Widmann, B., Badertscher, L., Zemp, I., Kozak, K., Csucs, G., Lund, E., and Kutay, U. (2010). A protein inventory of human ribosome biogenesis reveals an essential function of exportin 5 in 60S subunit export. PLoS Biol. 8, e1000522.

Wise, D.R., and Thompson, C.B. (2010). Glutamine addiction: a new therapeutic target in cancer. Trends Biochem. Sci. 35, 427–433.

Woolford, J.L., Jr., and Baserga, S.J. (2013). Ribosome biogenesis in the yeast Saccharomyces cerevisiae. Genetics 195, 643–681.

Wyler, E., Zimmermann, M., Widmann, B., Gstaiger, M., Pfannstiel, J., Kutay, U., and Zemp, I. (2011). Tandem affinity purification combined with inducible shRNA expression as a tool to study the maturation of macromolecular assemblies. RNA 17, 189–200.

Yuneva, M., Zamboni, N., Oefner, P., Sachidanandam, R., and Lazebnik, Y. (2007). Deficiency in glutamine but not glucose induces MYC-dependent apoptosis in human cells. J. Cell Biol. 178, 93–105.

Zemp, I., Wild, T., O'Donohue, M.F., Wandrey, F., Widmann, B., Gleizes, P.E., and Kutay, U. (2009). Distinct cytoplasmic maturation steps of 40S ribosomal subunit precursors require hRio2. J. Cell Biol. 185, 1167–1180.

Zemp, I., Wandrey, F., Rao, S., Ashiono, C., Wyler, E., Montellese, C., and Kutay, U. (2014). CK1δ and CK1ε are components of human 40S subunit precursors required for cytoplasmic 40S maturation. J. Cell Sci. 127, 1242–1253.

Zhang, J.H., Chung, T.D., and Oldenburg, K.R. (1999). A Simple Statistical Parameter for Use in Evaluation and Validation of High Throughput Screening Assays. J. Biomol. Screen. 4, 67–73.